Title:

In vitro and *in vivo* activation of astrocytes by amyloid β is potentiated by pro-oxidant agents

Authors and affiliation:

S García-Matas[1], N de Vera[1], A Ortega Aznar[2], JM Marimon[3], A Adell[4], AM Planas[1], R Cristòfol[1], C Sanfeliu[1].

1. Dept. Isquèmia Cerebral i Neurodegeneració, Institut d'Investigacions Biomèdiques de Barcelona (IIBB), CSIC-IDIBAPS, E-08036 Barcelona, Spain.
2. Dept. Anatomia Patològica (Neuropatologia), Hospital Universitari Vall d'Hebron, E-08035 Barcelona.
3. Unitat d'Experimentació Animal de Psicologia, Universitat de Barcelona, E-08035 Barcelona.
4. Departament de Neuroquímica i Neurofarmacologia, IIBB, CSIC-IDIBAPS, E-08036 Barcelona.

Running title:

Amyloid β activated astrocytes

Correspondence:

Dr Coral Sanfeliu
Dept. Brain Ischemia and Neurodegeneration
IIBB, CSIC-IDIBAPS
c/Rosselló 161, 6th floor
08036 Barcelona, Spain
Tel. (+34) 933638338
Fax. (+34) 933638301
coral.sanfeliu@iibb.csic.es

Abstract:

Alzheimer's disease (AD) is a devastating age-related neurodegenerative disease. Age is main risk factor for sporadic AD, which is the most prevalent type. Amyloid-β peptide (Aβ) neurotoxicity is the proposed first step in a cascade of deleterious events leading to AD pathology and dementia. Glial cells play an important role in these changes. Astrocytes provide vital support to neurons and modulate functional synapses. Therefore, the toxic effects of Aβ on astrocytes promote neurodegenerative changes that could lead to AD. Aging reduces astrocyte antioxidant defense and induces oxidative stress. We studied the effects of $A\beta_{42}$ on cultures of human astrocytes in the presence or absence of the following pro-oxidant agents: buthionine sulfoximine (BSO), a glutathione synthesis inhibitor, and $FeSO_4$, which liberates redox active iron. Pro-oxidant conditions potentiated Aβ toxicity, as shown by the generation of free radicals, inflammatory changes and apoptosis. A similar treatment was assayed in rats *in vivo*. A combination of $A\beta_{40}$ and $A\beta_{42}$ or $A\beta_{42}$ alone was infused intracerebroventricularly for 4 weeks. Other animal groups were also infused with BSO and $FeSO_4$. A long-term analysis that ended 4 months later showed higher cognitive impairment in the Morris water maze task, which was induced by Aβ plus pro-oxidant agent treatments. Pro-oxidant agents also potentiate brain tissue pathology. This was demonstrated in histological studies that showed highly increased astrocyte reactivity in AD-vulnerable areas, Aβ deposits and oxidative damage of AD-sensitive hippocampal neurons. To increase understanding of AD, experimental models should be used that mimic age - related brain changes, in which age-related oxidative stress potentiates the effects of Aβ.

Key words: human astrocyte cultures, rat model of Alzheimer's disease, amyloid-β peptide, iron, oxidative stress, inflammation

Introduction

Alzheimer's disease (AD) is the main age-related neurodegenerative disease. Despite intensive research, its trigger mechanisms are elusive and no cure is available yet. At present, the most widely accepted theory is the amyloid cascade hypothesis which postulates a brain increase in amyloid-β peptide (Aβ) as the main causative agent of a cascade of molecular and cellular events leading to neurodegeneration and dementia [1]. Genetic and environmental influences induce an excess of Aβ generation by sensitive neurons during the metabolism of its precursor protein. Both intracellular and extracellular Aβ cause a number of interrelated derangements, including inflammation, facilitation of tau hyperphosphorylation, disruption of mitochondrial and proteasomal function, oxidative stress, alteration of calcium signaling and impairment of synaptic function [2, 3]. The main pathological hallmarks of the disease, amyloid plaques and fibrillary tangles, together with neuronal loss, are considered the ultimate consequences of this cascade of events.

In sporadic AD, which accounts for 95 % of AD cases, the main risk factor is age. Age also has an influence on familial AD, as the disease always occurs during late maturity. There is likely to be an interaction between cell environment, metabolism of amyloid-β protein precursor (AβPP) and Aβ accumulation in AD throughout brain aging. One possible environmental influence is oxidative stress. Harman's free radical theory of aging [4] established the basis for discovering how oxidative damage accumulates in cells and leads to their deterioration with advancing age. Neurons are highly sensitive to oxidative damage because they have high metabolic activity, a high content of polyunsaturated fats and other oxidizable substrates, and relatively low antioxidant defenses [5]. This sets the conditions for increased Aβ generation in selectively vulnerable neurons in the aging brain. Pro-oxidant or oxidant agents have been shown to generate Aβ by increasing β-secretase and γ-secretase activity [6-9]. However, Aβ itself can induce the production of hydrogen peroxide or other reactive oxygen species (ROS) in concert with the redox active metal ions Fe^{2+} or Cu^{+} [10,11]. Iron and other biometals such as copper and zinc interact with Aβ and cause its aggregation [12,13]. Iron also interacts with AβPP at the translational level, as AβPP is post-transcriptionally regulated by iron regulatory proteins (IRPs) through a 5'UTR iron-responsive element (IRE) [14]. In brain aging, there is dysregulation of metal homeostasis and metals may accumulate in brain areas that are prone to neurodegeneration, which influences AD

pathology [11, 15-17]. Accumulated iron in the AD brain appears to contribute significantly to the oxidative damage that is one of the earliest pathological changes in AD [18, 19].

In addition to neurons, astroglia are major components of the brain. Astrocytes have an important role, beyond the provision of metabolic and structural support for neurons.They are involved in Ca^{2+} signaling, gliotransmission and modulation of synaptogenesis [20-22]. Their involvement in cognitive brain function, either through neuronal support function or by direct information processing in the tripartite synapsis [23], adds relevance to their role in AD development. We previously demonstrated that aged astrocytes *in vitro* and astrocytes cultured from the senescence-accelerated mouse model SAMP8 have higher oxidative stress, lower antioxidant defense and a decreased capacity to support neuron survival [24, 25]. In addition, we detected proteomic changes that are indicative of brain AD-like functional deterioration in both astrocytes and neurons from SAMP8 [26]. Therefore, aged astrocytes may not effectively defend neurons against the development of AD. Indeed, Aβ triggers a neuroprotective response in healthy astrocytes, which involves either phagocytosis and degradation of Aβ [27] or increased secretion of neuroprotective factors [28, 29]. In contrast, aged astrocytes may have deficits in Aβ clearance and neurotrophic support and may even secrete pro-inflammatory agents, derived from their basal level of activation [30]. Accordingly, astrocytes from SAMP8 mice showed a higher level of reactive gliosis after $A\beta_{42}$ treatment than cultures from non-senescent mice [31].

The aim of this study was to analyze how increased oxidative stress in the aging brain contributes to the development of AD pathology, with an emphasis on astrocytes. Human astrocyte cultures were used as an *in vitro* model to study the astrocyte response to $A\beta_{42}$ in a pro-oxidant environment. This environment was created by glutathione depletion with buthionine sulfoximine (BSO) and the redox active iron compound $FeSO_4$. Next, we used a validated AD rat model with a four-week chronic intracerebroventricular (icv) infusion of a mixture of $A\beta_{40}$ and $A\beta_{42}$ [32]. In this *in vivo* model, we assayed the long-term effects of glutathione depletion and reactive iron with Aβ, BSO and $FeSO_4$ doses according to a previous short-term study [33].

Materials and methods

Human astrocyte cultures

Human cortical brain tissue was obtained from normal, legally aborted fetuses at 14-16 weeks of gestation. Permission to use human fetal tissue was obtained from the ethics committee of the Spanish National Research Council (CSIC). Cultures of human cerebral cortical astrocytes were prepared as described elsewhere [34]. Cell culture media and reagents were purchased from Gibco (Invitrogen, Paisley, United Kingdom). Plastic culture plates were from Nunc (Roskilde, Denmark). Briefly, after enzymatic digestion and dissociation of tissue samples, cells were suspended in minimum Eagle's medium (MEM) supplemented with 5% heat-decomplemented horse serum, 0.5% w/v D-glucose, 2 mM glutamine 200 µg/mL gentamycin and 0.5 µg/L fungizone. Cells were seeded in poly-L-lysine-coated culture plates and maintained in a humidified CO_2 incubator at 37ºC. Fresh medium was added weekly until the end of the study. To obtain highly enriched astrocyte cultures, cells were seeded at 2-3x10^6 cells/ml and submitted to limited *in vitro* passage. For this purpose, 1 month old cultures were extensively washed with PBS, mildly trypsinized in the presence of 0.02% EDTA, and reseeded at 1x10^6 cells/ml. Another passage was performed 2 weeks later. Alternatively, primary cultures were frozen in liquid nitrogen (cryoprotected with 10% DMSO in serum) at the first passage, and thawed later on to grow the highly enriched astrocyte cultures. Astrocytes were seeded for experiments at 0.5x10^6 cells/ml (1.5x10^5 cells/cm^2) in 96-well plates and used after 2-3 days. Cultures consisted of 90–95% astrocytes, 5–10% microglia and 0.1–1% oligodendroglia as reported elsewhere [34]. All reagents used in the study were from Sigma-Aldrich, Inc. (St. Louis, MO), unless otherwise stated.

Hydroperoxide generation assay

Oxidative stress in astrocyte cultures was studied using 2',7'-dichlorofluorescein diacetate (DCFH-DA, Molecular Probes, Invitrogen) to determine intracellular hydroperoxide generation [34]. The non-fluorescent probe DCFH-DA freely permeates the cell membrane. Once the DA Group has been hydrolyzed by cell esterases, DCFH may be oxidized to the fluorescent 2',7'-dichlorofluorescein (DCF). Either control cultures or cultures that had been pre-incubated 24 h with BSO 1mM were washed in HEPES and loaded with 10 µM of DCFH-DA from a stock solution of 2 mM in methanol. After 20 min of incubation at 37ºC cells were washed again in HEPES and basal fluorescence was measured at 485 nm excitation/530 nm emission in a plate reader (Spectramax Gemini XS, Molecular Devices, MDS, Sunnivale, CA). Then, the

agents $FeSO_4$ and $A\beta_{42}$ were added to the corresponding wells at concentrations of 25 μM and 20 μM, respectively. BSO was added to the pre-incubated wells when the probe was loaded and during the incubation with $FeSO_4$ and $A\beta_{42}$. Fibrillar $A\beta_{42}$ was dissolved in DMSO [35]. The corresponding controls were incubated with the vehicle. After 4 h, fluorescence was measured again. The increase in intracellular ROS was quantified from a standard curve of DCF in methanol (0.5-100 nM) and expressed as the DCF generated per μg of protein. The concentration of proteins was determined by the Bradford method. Aβ peptides in the study were from Bachem (Bubendorf, Switzerland).

Nitrite assay

Nitric oxide synthesis by activated astrocyte cultures was measured by the colorimetric Griess reaction that detects nitrite (NO_2^-), a stable reaction product of nitric oxide (NO) and molecular oxygen. Astrocytes were treated with 10 ng/ml of interleukin-1β, 10 ng/ml of interferon-γ, or both. Next, experiments were performed with 1 mM BSO, 10 μM $FeSO_4$ and 5 μM $A\beta_{42}$. Whenever present, BSO was additionally preincubated for 24 h. Agents were directly added to the culture media in the wells. After 3 days of exposure to the treatments, 50 μL aliquots of culture supernatants were incubated with 50 μL Griess reagent (1% sulphanilamide, 0.1% N-(1-naphthyl)ethylenediamine dihydrochloride and 5% phosphoric acid) at room temperature for 10 min and the optical density at 540 nm was then determined using a microplate reader (iEMS Reader MF, Labsystems, Finland). The nitrite concentration was determined from a sodium nitrite standard curve (1-50 μM).

Immunocytochemistry and cell death staining

Morphological changes caused by exposure to cytokines or to BSO, $FeSO_4$, and $A\beta_{42}$ for 3 days were analyzed in astrocytes that were immunostained with anti-glial fibrillary acidic protein (GFAP, Dako, Glostrup, Denmark). For that purpose, astrocyte cultures were fixed with 4% paraformaldehyde, permeabilized with 0.2 % Triton X-100, and incubated with 3% normal goat serum to block nonspecific binding. Cultures were incubated overnight with the primary antibody at a dilution of 1:5000 in the presence of 1.5% blocking serum. The cells were washed and incubated with Alexa Fluor 488-conjugated secondary antibody (1:1500; Molecular Probes, Invitrogen) for 1 h. In

addition, cell nuclei were stained with bisbenzimide (5 μM). The number of normal nuclei and that of condensed and fragmented nuclei, which are indicative of apoptosis, was counted with the analySIS image analysis software (Soft Imaging System, Münster, Germany). At least two fields (1.3 mm^2 / field) were microphotographed for each well.

Animals and treatments

Male 3-month-old Sprague-Dawley rats that had been retired from breeding and weighed 300-350 g were purchased from Charles River (Lyon, France). They were kept at the University of Barcelona's animal facility in standard conditions of temperature and humidity, with two animals per cage, a 12-h light, 12-h dark cycle, and food and water *ad libitum*. All handling and experimental procedures were approved by the Animal Ethics and Health Committees of the University of Barcelona.

Rats were infused icv for 4 weeks through an osmotic pump (see Surgical procedures) either with vehicle, pro-oxidant compounds, Aβ or a combination of pro-oxidants and Aβ. The pro-oxidant treatment was a mixture of $FeSO_4$ and BSO at the doses reported previously [33]. Aβ was administrated as a mixture of $A\beta_{40}$ and $A\beta_{42}$ in human high density lipoprotein (HDL) as a carrier, with a previous injection of 10 ng transforming growth factor β1 (TGFβ1) (R&D Systems, Minneanapolis, MN) into both anterodorsal thalamus nuclei, according to the *in vivo* rat model established by Frautschy and cols. [32]. The vehicle was HEPES 4 mM, pH 8. An additional group with the combination of pro-oxidants and a high dose of $A\beta_{42}$ was added as a reference [33]. Therefore, rats were randomly assigned to one of five separate groups (6-8 animals per group): Group I, vehicle; Group II, 0.47 mg $FeSO_4$ heptahydrate (1.68 μmol $FeSO_4$) and 4.48 mg (20.16 μmol) BSO; Group III, 20 μg (10.1 nmol) $A\beta_{40}$ and 30 μg (15.1 nmol) $A\beta_{42}$ in 80 μg HDL; Group IV, $FeSO_4$/BSO plus $A\beta_{40}$/$A\beta_{42}$; Group V, $FeSO_4$/BSO plus 50 μg (25.2 nmol) $A\beta_{42}$. The mixture of BSO and $FeSO_4$ was prepared in distilled water and administrated in a separate pump from Aβ to avoid chemical interactions. The indicated doses are the total received at the end of the infusion period. The perfusion rate of the pumps was 0.25 μl/h. All animals were subjected to brain histological studies after completion of the long-term behavioral studies, as described below. Three or four animals per group were added to the study to be sacrificed immediately after the brain infusion treatment and analyzed by brain histology.

Surgical procedures

Rats were anesthetized with a mixture of ketamine 80 mg/kg (Ketolar 50 mg/ml®, Pfizer, Alcobendas, Madrid, Spain) and xylazine 5 mg/kg (Rompun®, Bayer, Kiel, Germany) that was intraperitoneally injected. Alzet model 2004 mini-osmotic pumps (Alzet Osmotic Pumps, Durect Corporation, Cupertino, CA), attached via polyethylene tubing to brain catheters (Alzet), were filled with the treatment solutions and stereotactically implanted into the lateral ventricles. Animals receiving pro-oxidants and Aβ and controls had one minipump implanted in each lateral ventricle. The stereotactic coordinates were: anterior-posterior (AP) and medio-lateral (ML) to bregma -0.9 mm and ± 1.4 mm, respectively; dorso-ventral (DV) to dural surface: -3.5 mm. Animals receiving TGFβ1 were injected immediately before pump implantation at the coordinates of the anterodorsal thalamus nuclei: AP -2.1 mm, ML ± 1.4 mm, and DV -4.6 mm, using a 25 G stainless steel cannula (Small Parts Inc, Miami, FL) connected to a Hamilton syringe through a Teflon tube. The syringe was attached to a micro-infusion pump (Bioanalytical systems Inc., West Lafayette, IN). The cannula was left in position for 5 min after delivery to prevent the solution from surging back. At the end of the 4-week infusion period, rats were slightly anesthetized to remove the osmotic pumps. Pump patency and functionality were confirmed by verifying that the pump contents had been discharged and that the infusion apparatus was intact.

Behavioral testing

The behavioral test for spatial learning memory was performed in a Morris water maze (MWM). The apparatus and procedures were basically as described elsewhere [36, 37]. The behavioral test was initiated 4 weeks after surgery when the treatment was complete. A pre-training test with no landmarks and a hidden platform consisted in 4 trials over 2 days. The rats were given 120 s to find the platform, and then allowed to remain on it for 30 s. Rats that did not reach the platform were picked up, placed on the platform and left there for 30 s. The procedure was the same in the acquisition test, but the animals had to rely on the landmarks to find the hidden platform. Animals were given 4 escape trials per day for 6 days, which amounted to a total of 24 trials. On the last day, a 60 s probe trial was performed with the platform removed. To analyze the rat's behavior, the surface of the pool was divided into four quadrants and the time that the rat spent in the quadrant where the platform had previously been located was calculated. To monitor long-term memory, animals were submitted to a new series of 2 escape trials followed by a 60 s probe trial at 1, 5 and 9 weeks after the end of the

acquisition period. Three weeks later, a new training acquisition assay of 4 escape trials per day for 6 days was performed with reversal of the location of the submerged platform. A 60 s probe trial with the platform removed was performed on the last day. New probe trials, preceded by 2 escape trials, were performed after 1, 2 and 4 weeks. The study ended 4 months after the infusion treatment.

Rat brain dissection and histology

Rats were anesthetized as described above and perfused with isotonic saline (0.9 % NaCl) with heparin, followed by isotonic saline and finally by buffered formaldehyde (4% formaldehyde in phosphate buffer 0.01 M pH 7.4). Brains were quickly removed, placed in a Stoelting Tissue Slicer and cut into 4 mm blocks. Tissue blocks were postfixed with buffered formaldehyde for 24 h, then washed with phosphate buffer for 24 h and finally washed with water. Next they were dehydrated and embedded in paraffin. Paraffin-embedded blocks were sectioned at 5-7 μm and mounted on Histogrip (Zymed laboratories, Invitrogen) coated slides for immunostaining. Paraffin-embedded sections were dewaxed in xylene and rehydrated through decreasing concentrations of ethanol before staining. The accuracy of the cannula placement was determined by hematoxylin or Nissl staining. Microglia immunostaining was carried out by free floating 50 μm vibratome sections of non-paraffin-embedded rat brains. Antigen retrieval was performed by boiling the sections in 10 mM citrate buffer (pH 6) for 10 min. When sections had cooled, they were washed in saponin 0.05% in PBS and then in PBS. Normal serum (horse or goat, 1:5) in 0.2 % gelatin, 0.2 % Triton X-100 in PBS was used at room temperature to block non-specific reactions for 2 h. Sections were incubated with the appropriate antibody diluted in 0.2 % Triton X-100 and normal serum (1:20) in PBS at 4ºC overnight. The following primary antibodies were used to detect specific brain tissue alterations: anti-Aβ clone 4G8 (1:150; Signet, Dedham, MA), anti-8-hydroxy-2'-deoxyguanosine (8OHdG) (1:50; JaICA, Nikken SEIL, Fukuroi, Japan), anti-GFAP (1:300; Dako), anti-ubiquitin (1:50; Novocastra, Newcastle upon Tyne, England) and anti-macrophage complement receptor 3 (OX42, 1:500; AbD Serotec, Kidlington, UK). Sections were then washed in PBS and incubated with the appropriate biotinylated secondary antibody for 2 h at room temperature. Tomato lectin histochemistry was carried out on paraffin-embedded sections overnight at 4°C using biotinylated lectin from *Lycopersicum esculentum* (2.5 μg/ml). The Vectastain ABC kit (Vector Laboratories, CA) was used as per manufacturer's instructions, and the reaction

was visualized with diaminobenzidine containing 0.1 % H_2O_2 for 5–10 min. Where required, sections were lightly counterstained with Harris' hematoxylin. Iron deposits were visualized by Pearl's Prussian blue staining and counterstaining with neutral red, following standard procedures. Selected paraffin sections were also stained with fluoro-Jade B (following the protocol of the supplier, Chemicon International) to check for degenerating neurons and reactive astroglia [38]. Then, the tissue sections were dried, dehydrated through increasing ethanol concentrations and xylene, and mounted in DPX (Fluka, Buchs, Switzerland). Selected sections of Aβ treated rats were also stained for Aβ deposits with thioflavine S (1 % thioflavine S aqueous solution staining) followed by 70º ethanol differentiation. Then they were mounted in Mowiol (Calbiochem, Merck, Darmstadt, Germany).

Data analysis

Results are shown as mean ± SEM. Statistics was performed with one way ANOVA and repeated measures ANOVA for *in vitro* and *in vivo* experiments, respectively. A post hoc Newman-Keuls test was used for group comparison (GraphPad Prism software, GraphPad, San Diego, CA).

Results

In vitro oxidative stress

Oxidative stress changes in human astrocyte cultures are shown in Fig.1. Depletion of glutathione by BSO did not increase the generation of hydroperoxides measured by DCFH-DA in normal culture conditions. Neither did Aβ exposure. The presence of oxidant ferrous ion from $FeSO_4$ induced a small increase in hydroperoxide generation. However, a highly significant increase in DCF fluorescence was detected when both pro-oxidant agent treatments, BSO and $FeSO_4$, were added to Aβ exposure.

In vitro inflammation

A three-day treatment with a mixture of interleukin-1β and interferon-γ induced morphological changes and NO generation in the human astrocytes, both of which are indicative of an inflammatory response (Fig. 2). Unstimulated astrocytes generally

exhibited a flattened and polygonal morphology, whereas activated astrocytes showed thinner and elongated cytoplasm processes and spherical nuclei in a stellate-like morphology. No changes were evident with interleukin-1β, but interferon-γ and the mixed treatment of both cytokines induced a characteristic stellate morphology with long cytoplasmic processes (Fig. 2 A-D). The presence of nitrite formation in the culture medium, which is indicative of NO astrocyte generation, was also significantly enhanced by the mixed cytokine treatment (Fig. 2 E). The peptide Aβ did not increase NO over control values (3.6 ± 0.2 μM), either alone (3.3 ± 0.4 μM) or in the presence of pro-oxidant agents (3.4 ± 0.3 μM). Therefore, we analyzed the presence of Aβ-induced morphological changes, which are indicative of inflammation, in comparison to changes after the cytokine treatment (Fig. 3). The combined treatment of BSO, $FeSO_4$ and Aβ caused a clear reorganization of the human astrocyte cytoskeleton, which was similar to that seen with cytokines. In contrast, Aβ alone caused moderate changes (Fig. 3 A-D).

***In vitro* cytotoxicity**

No cytotoxicity was caused by BSO treatment or exposure to $FeSO_4$ or Aβ alone in human astrocytes. However, a small increase in condensed nuclei which are indicative of apoptotic cell death, was detected after the combined treatment of BSO, $FeSO_4$ and Aβ (Fig 3 D and E).

***In vivo* toxicity**

The treatment administrated to Group IV (BSO/ $FeSO_4$ plus $A\beta_{42}/A\beta_{40}$), was highly toxic. Two out of 8 rats died during the experiment (and were excluded from the the behavioral results). Rats in this group had more dilated cerebral ventricles than the other animals, which suggests that they had impaired CSF drainage.

Cognitive deterioration

The time spent in the water maze quadrant where an escape platform has been located is a reliable indicator of rat learning and memory capacities in our experimental conditions, as discussed elsewhere [37]. Results of the probe trials for the different treatment groups are shown in Fig. 4. Rats infused with BSO and $FeSO_4$ showed learning acquisition, a pattern of retention and a post-acquisition period that did not differ from that of the control animals (Fig. 4A). When the platform position was

changed (Fig. 4B), no differences were detected between rats treated with pro-oxidant agents and the control group. All the Aβ-treated groups had significantly decreased learning and memory (Fig. 4A and B). Reversel acquisiton clearly evidenced lower cognitive capacities in groups treated with the mixture of BSO/$FeSO_4$ and Aβ, when either a mixture of $A\beta_{40}$ and $A\beta_{42}$ [32] was administered or a higher dose of $A\beta_{42}$ [33] (Fig. 4B).

Histological alterations

Rats receiving Aβ (Groups III, IV and V) showed brain tissue deposits that stained positive for anti-Aβ antibody. Groups IV and V, in which rats were infused with BSO/ $FeSO_4$ in addition to Aβ, had much higher deposition than those in Group III. Diffuse plaques or precipitates were preferentially detected in areas next to the infused ventricle, such as corpus callosum and septum, but also in cerebral cortex, vessels and all over the brain. Aβ deposits were present in rats that were either immediately sacrificed after infusion or sacrificed at 4 months post-infusion. Brain septum presented a high density of Aβ precipitates mainly in Group IV. The septum is a cellular area in the rat, which contains neuron complexes highly interconnect with the hippocampus [39]. As expected, Aβ precipitates stained positive for thioflavine S (not shown). Representative histological images are shown in Fig. 5.

We did not detect iron precipitates in the brain tissue of rats from Groups I, II and III. Ferric iron was barely detected in the hippocampus, septum or other areas next to the infused ventricle of rats treated with the mixture of BSO/$FeSO_4$ and Aβ (mainly Group V), which were sacrificed after infusion. Four months later, Group IV showed extensive iron staining. See representative histological images in Fig. 6.

Hypertrophic astrocytes that were highly reactive to anti-GFAP were mainly detected in rat Groups IV and V in the hippocampus, corpus callosum and frontal cortex. Inflammatory effects were detected at the end of the infusion and continued throughout the 4 months post-infusion. In the long term, Group IV astrocytes were more reactive than Group V. Fluoro-Jade B distinctly stained the most reactive astrocytes that were those in Group V rats sacrificed immediately after the infusion. Representative histological images are shown in Fig. 7.

Inflammatory effects were also shown by the presence of reactive microglia that were stained with anti-OX42 stain, mainly in the Group IV rats. Lectin staining showed more

ramified microglia in Aβ-treated groups. In the long term, Group IV rats still showed reactive microglia. Representative images are shown in Fig. 8.

No neuron damage was histologically detected in the rats sacrificed immediately after the pump-infusion, but alterations were detected in rats sacrificed at the end of the 4 month post infusion study. Oxidative DNA damage, as indicated by anti-8OHdG staining was high in Group IV and less extensive in Group V. It occurred mainly in hippocampal pyramidal neurons. Intraneuronal accumulation of ubiquitin and ubiquitinated proteins, as stained by the anti-ubiquitin antibody, was detected in neurons of the hippocampus and cortex of rats from Groups III and IV and was less intense in Group V. DNA oxidation was present in pyramidal neurons, whereas ubiquitin accumulation also occurred in other neuron types. Representative images are shown in Fig. 9.

Discussion

Astrocytes are generally more resistant to toxins than neurons, but they are exposed to Aβ damage. It is known that human astrocytes *in vitro* can bind and internalize $A\beta_{42}$ [40, 41], as they do *in vivo*. In this work, *in vitro* incubation with $A\beta_{42}$ induced poor toxic effects in human astrocytes, as seen by the absence of oxidative stress and cell death. Only slight morphological changes were appreciable, indicating some activation effect. This confirms a previous report in which cultures of human astrocytes were not killed by $A\beta_{40}$ or $A\beta_{42}$, even when it was intracellularly microinjected [42]. However, aggregated $A\beta_{40}$ was toxic to up to 50 % of the cultured rat astrocytes, probably through the generation of hydrogen peroxide [43], a major Aβ neurotoxicity mechanism [44]. Changes in intracellular Ca^{2+} signaling leading to mitochondrial impairment, oxidative stress and glutathione depletion were also reported in rat astrocyte cultures and caused by specific insertion of β-aggregated $A\beta_{42}$ into the astrocyte plasma membrane [45]. Therefore rat astrocytes are more vulnerable to Aβ than human astrocytes *in vitro*, even though Aβ probably induces oxidative stress in human astrocytes. In this case, Aβ toxicity would increase in a pro-oxidant environment with lower antioxidant defense. Certainly, the toxic and inflammatory damage to human astrocytes caused by $A\beta_{42}$ increased greatly in the presence of redox active iron and an inhibitor of glutathione synthesis. As expected, depletion of glutathione *per se* did not induce

oxidative stress, whereas Fe^{2+} and BSO/Fe^{2+} increased ROS generation but not cell death. The pro-oxidative effects of BSO and Fe^{2+} partially mimic the oxidative stress of aged brain astrocytes, with lower antioxidant defense and free radical damage [24, 25]. The age-related iron homeostasis disruption leads to iron increase and also contributes to oxidative stress in the aged brain [15]. Incubation of cultured human astrocytes with $A\beta_{42}$ induced negligible ROS generation, which was highly significant in aged-like astrocytes, with impaired antioxidant defense and Fe^{2+}-induced oxidative stress.

Human astrocytes *in vitro* show flat and polygonal morphology, even though they are multiple branched cells in the brain. This is also the case for murine astrocyte cultures. In the latter, several agents, including cytokines and Aβ, induce skeletal reorganization to a stellate morphology, which is indicative of activation plastic changes [46-48]. Treatment with IL1β induced a stellate morphology in our human astrocyte cultures, as previously reported by other authors [49]. To a lesser extent, Aβ exposure caused morphological changes that are indicative of activation. These changes were highly potentiated in a pro-oxidant environment when the peptide was co-incubated with $FeSO_4$ in glutathione-depleted astrocytes. We did not detect an increase in nitrite formation after these treatments. Activated astrocytes adjacent to Aβ plaques in AD brain generate NO [50], whereas astrocytes in healthy brain do not. The astrocyte inducible enzyme NO synthase is activated by cytokines or other mediators of brain damage. Several authors have reported that Aβ causes NO generation in murine astrocyte cultures in the presence of cytokines, that are either co-incubated [51] or released by contaminating microglia [52]. However, the peptide alone does not cause NO generation [53; but see 54]. We found that cultured human astrocytes generated NO after incubation with cytokines, but not with Aβ. The mixture of IL1β and INFγ produced nitrite, as previously described [55, 56].

The mixed treatment of $A\beta_{42}$ plus BSO and Fe^{2+} induced a low level of apoptotic death, which corroborates its toxic effects. An apoptotic pathway was also reported in cultured rat astrocytes, as induced by Aβ toxicity [57]. The increased sensitivity of human astrocytes to Aβ in the presence of iron and impaired redox homeostasis means that aged astrocytes are more liable to suffer Aβ damage and enter into the AD vicious cycle of oxidative stress and inflammation than those in young individuals. Thus, aged astrocytes no longer carry out their functions of synapsis modulation and vital support to neurons. Instead, they contribute to AD pathophysiology.

The icv infusion of Aβ in rat is a widely used AD model for pharmacological studies, as cognitive impairment and other AD-related pathologies can be reliably quantified [58, 59]. The 4-week combined $A\beta_{40}/A\beta_{42}$ infusion in a model developed by Frautschy and cols. causes gliosis, deposition of Aβ and delayed cognitive impairment [32]. It has been suggested that infused $A\beta_{42}$ induces oxidative stress and astrocytic dysfunction that are in the basis of the learning deficits [60]. Accordingly, we found a sustained decrease of cognitive abilities in the MWM. Twelve weeks after the first training, retention of reversal platform training was lower than in the control group, which indicated that long-term cognitive loss had occurred. Moderate AD related brain pathology was observed, as previously reported [32]. The infusion of a pro-oxidant treatment with BSO and Fe^{2+} did not show toxic effects *per se* throughout the entire study. However, when treatments $A\beta_{40}/A\beta_{42}$ plus BSO/Fe^{2+} were simultaneously administrated, both behavioral and pathological studies showed increased toxicity. These rats had a similar, behaviorally impaired response to the $A\beta_{40}/A\beta_{42}$ treated rats in the first training, but a worse response in late reversal training. Histologically, Aβ deposits were highly increased, astrocytes were more reactive at the end of the treatment and they partially maintained activation throughout the 4-month study. Microglia was more reactive and iron deposits were present until the end of the study. As regards neurons, hippocampus pyramidal neurons showed highly oxidized DNA at 4 months after $A\beta_{40}/A\beta_{42}$ plus BSO/Fe^{2+}, whereas intraneuronal ubiquitin accumulation was similar to that caused by $A\beta_{40}/A\beta_{42}$ treatment. Thus, in this rat model, Aβ inhibits the neuronal ubiquitin proteasome system, as reported in AD patients [61, 62].

We knew from a previous study that post-acquisition icv infusion with $A\beta_{42}$ alone plus BSO and Fe^{2+} induced decreased performance in the MWM tested immediately after the treatment [33]. When we tested this treatment in our long-term study, we found a long lasting spatial memory impairment, similar to that of the group treated with $A\beta_{40}/A\beta_{42}$ plus BSO/Fe^{2+}. Even though both rat groups were similarly impaired behaviorally, AD pathology was more intense in rats infused with $A\beta_{40}/A\beta_{42}$ and BSO/ Fe^{2+} than in those with $A\beta_{42}$ and BSO/ Fe^{2+}. This could be partially related to the fact that iron deposits were long lasting in the first but not in the second group, where they could only be detected in rats sacrificed immediately after infusion. Therefore, the interaction of iron with different Aβ species can modulate the pathological outcome. It seems that a

mixture of 20 μg of $A\beta_{40}$ plus 30 μg of $A\beta_{42}$ [32] can lead to longer lasting effects *in vivo* than 50 μg of $A\beta_{42}$ alone [33].

In AD, redox active iron has been reported both intraneuronally in vulnerable neurons [63] and associated with amyloid plaques and neurofibrillary tangles [64]. Iron was also increased in the Aβ deposits of AD transgenic mice [65]. In our study we detected an inflammatory response in the astrocytes of rats treated with iron and Aβ, which parallels the *in vitro* effects discussed above in human astrocytes. The increased oxidative stress seen in these rat hippocampal neurons may be partially derived from the impaired antioxidant capacity of the surrounding astrocytes. Early Aβ-induced astrocyte derangements may contribute to neuron death by failure of antioxidant support [66]. In advanced stages of AD pathology, these chronic astrocyte alterations of oxidative stress and inflammation will further impair neuron functionality and contribute to the degenerative process [67, 68].

Overall we gathered *in vitro* and *in vivo* data that further confirm the involvement of redox reactive iron in the development of age-related AD pathology and suggest early Aβ damage of frail, aged astrocytes. Therefore, the use of *in vitro* and *in vivo* aging models may help to understand the brain aging contribution to AD development and progression. In this line, Pallas and cols. have suggested that the use of the previously mentioned SAMP8, senescent mice with some incipient AD traits, may help to unveil "the switch" from aging to AD [69].

Acknowledgments

This study was supported by grants SAF2006-13092-C02-02 from the Spanish Ministerio de Ciencia e Innovación, RD06/0013/1004 (RETICEF) from the Instituto de Salud Carlos III, 062931 from Fundació La Marató de TV3 and by the European Network of Excellence DiMI (LSHB-CT-2005-512146). S García-Matas received a Generalitat (Autonomous Government of Catalonia) fellowship. We thank MA Marqués, J López Regal and A Parull for their skilful technical assistance. We thank Dr T Rodrigo for her assistance in the behavioral studies. We gratefully acknowledge Y Trejo, R López and Dr S Barambio from Tutor Médica Clinics (Barcelona) for providing the donated human tissue. The authors declare that there are no financial or commercial conflicts of interest.

References

[1] Selkoe DJ (2002) Alzheimer's disease is a synaptic failure. *Sience* **298**, 789-791.

[2] Verdile G, Fuller S, Atwood CS, Laws SM, Gandy SE, Martins RN (2004) The role of beta amyloid in Alzheimer's disease: still a cause of everything or the only one who got caught? *Pharmacol Res* **50**, 397-409.

[3] LaFerla FM, Green KN, Oddo S (2007) Intracellular amyloid-β in Alzheimer's disease. *Nature Rev* **8**, 499-509.

[4] Harman, D (1956) Aging: a theory based on free radical and radiation chemistry. *J Gerontol* **11**, 298–300.

[5] Halliwell B (2006) Oxidative stress and neurodegeneration: where are we now? *J Neurochem* **97**, 1634-1658.

[6] Tamagno E, Bardini P, Obbili A, Vitali A, Borghi R, Zaccheo D, Pronzato MA, Danni O, Smith MA, Perry G, Tabaton M (2002) Oxidative stress increases expression and activity of BACE in NT2 neurons. *Neurobiol Dis* **10**, 279-288.

[7] Tamagno E, Guglielmotto M, Aragno M, Borghi R, Autelli R, Giliberto L, Muraca G, Danni O, Zhu X, Smith MA, Perry G, Jo DG, Mattson MP, Tabaton M (2008) Oxidative stress activates a positive feedback between the gamma- and beta-secretase cleavages of the beta-amyloid precursor protein. *J Neurochem* **104**, 683-695.

[8] Shen C, Chen Y, Liu H, Zhang K, Zhang T, Lin A, Jing N (2008). Hydrogen peroxide promotes Aβ production through JNK-dependent activation of γ-secretase. *J Biol Chem* **283**, 17721-17730.

[9] Jin SM, Cho HJ, Jung ES, Shim MY, Mook-Jung I (2008) DNA damage-inducing agents elicit gamma-secretase activation mediated by oxidative stress. *Cell Death Differ* **15**, 1375-1384.

[10] Khan A, Dobson JP, Exley C (2006) Redox cycling of iron by $A\beta_{42.}$ *Free Radic Biol Med* **40**, 557-569.

[11] Liu G, Huang W, Moir RD, Vanderburg CR, Lai B, Peng Z, Tanzi RE, Rogers JT, Huang X (2006) Metal exposure and Alzheimer's pathogenesis. *J Struct Biol* **155**, 45-51.

[12] Huang X, Atwood CS, Moir RD, Hartshorn MA, Tanzi RE, Bush AI (2004) Trace metal contamination initiates the apparent auto-aggregation, amyloidosis, and oligomerization of Alzheimer's Aβ peptides. *J Biol Inorg Chem* **9**, 954-960.

[13] Exley C (2006) Aluminium and iron, but neither copper nor zinc, are key to the precipitation of β-sheets of $A\beta_{42}$ in senile plaque cores in Alzheimer's disease. *J Alzheimers Dis* **10**, 173-177.

[14] Rogers JT, Bush AI, Cho HH, Smith DH, Thomson AM, Friedlich AL, Lahiri DK, Leedman PJ, Huang X, Cahill CM (2008) Iron and the translation of the amyloid precursor protein (APP) and ferritin mRNAs: riboregulation against neural oxidative damage in Alzheimer's disease. *Biochem Soc Trans* **36**, 1282-1287.

[15] Zecca L, Youdim MB, Riederer P, Connor JR, Crichton RR (2004) Iron, brain ageing and neurodegenerative disorders. *Nature Rev* **5**, 863-873.

[16] Adlar PA, Bush AI (2006) Metals and Alzheimer's disease. *J Alzheimers Dis* **10**, 145-163.

[17] Zhu WZ, Zhong WD, Wang W, Zhan CJ, Wang CY, Qi JP, Wang JZ, Lei T (2009) Quantitative MR 2009 Phase-corrected Imaging to Investigate Increased Brain Iron Deposition of Patients with Alzheimer Disease. *Radiology* **253**, 497-504.

[18] Casadesus G, Smith MA, Zhu X, Aliev G, Cash AD, Honda K, Petersen RB, Perry G (2004) Alzheimer disease: Evidence for a central pathogenic role of iron-mediate reactive oxygen species. *J Alzeimers Dis* **6**, 165-169.

[19] Zhu X, Su B, Wang X, Smith MA, Perry G (2007) Causes of oxidative stress in Alzheimer disease. *Cell Mol Life Sci* **64**, 2202-2210.

[20] Elmariah SB, Hughes EG, Oh EJ, Balice-Gordon RJ (2005) Neurotrophin signaling among neurons and glia during formation of tripartite synapses. *Neuron Glia Biol* **1**, 1-11.

[21] Halassa MM, Fellin T, Haydon PG (2007) The tripartite synapse: roles for gliotransmission in health and disease. *Trends Mol Med* **13**, 54-63.

[22] Perea G, Navarrete M, Araque A (2009) Tripartite synapses: astrocytes process and control synaptic information. *Trends Neurosci* **32**, 421-431.

[23] Araque A, Parpura V, Sanzgiri RP, Haydon PG. (1999) Tripartite synapses: glia, the unacknowledged partner. *Trends Neurosci* **22**, 208-215.

[24] Pertusa M, García-Matas S, Rodríguez-Farré E, Sanfeliu C, Cristòfol R (2007) Astrocytes aged in vitro show a decreased neuroprotective capacity. *J Neurochem* **101**, 794-805.

[25] García-Matas S, Gutierrez-Cuesta J, Coto-Montes A, Rubio-Acero R, Díez-Vives C, Camins A, Pallàs M, Sanfeliu C, Cristòfol R (2008) Dysfunction of astrocytes in

senescence-accelerated mice SAMP8 reduces their neuroprotective capacity. *Aging Cell* **7**, 630-640.

[26] Díez-Vives C, Gay M, García-Matas S, Comellas F, Carrascal M, Abian J, Ortega-Aznar A, Cristòfol R, Sanfeliu C (2009) Proteomic study of neuron and astrocyte cultures from senescence-accelerated mouse SAMP8 reveals degenerative changes. *J Neurochem* **111**, 945-955.

[27] Wyss-Coray T, Loike JD, Brionne TC, Lu E, Anankov R, Yan F, Silverstein SC, Husemann J. (2003) Adult mouse astrocytes degrade amyloid-β in vitro and in situ. *Nat Med* **9**, 453-457.

[28] Ramírez G, Toro R, Döbeli H, von Bernhardi R (2005) Protection of rat primary hippocampal cultures from A beta cytotoxicity by pro-inflammatory molecules is mediated by astrocytes. *Neurobiol Dis* **19**, 243-254.

[29] Kimura N, Takahashi M, Tashiro T, Terao K (2006) Amyloid β up-regulates brain-derived neurotrophic factor production from astrocytes: rescue from amyloid β-related neuritic degeneration. *J Neurosci Res* **84**, 782-789.

[30] Yu WH, Go L, Guinn BA, Fraser PE, Westaway D, McLaurin J (2002) Phenotypic and functional changes in glial cells as a function of age. *Neurobiol Aging* **23**, 105-115.

[31] Lü L, Mak YT, Fang M, Yew DT (2009) The difference in gliosis induced by beta-amyloid and Tau treatments in astrocyte cultures derived from senescence accelerated and normal mouse strains. *Biogerontology* in press, DOI: 10.1007/s10522-009-9217-3.

[32] Frautschy SA, Hu W, Kim P, Miller SA, Chu T, Harris-White ME, Cole GM (2001) Phenolic anti-inflammatory antioxidant reversal of Aβ-induced cognitive deficits and neuropathology. *Neurobiol Aging* **22**, 993–1005.

[33] Lecanu L, Greeson J, Papadopoulos (2006) Beta-amyloid and oxidative stress jointly induce neuronal death, amyloid deposits, gliosis, and memory impairment in the rat. *Pharmcology* **76**, 19-33.

[34] Sebastià J, Cristòfol R, Pertusa M, Vílchez D, Torán N, Barambio S, Rodríguez-Farré E, Sanfeliu C (2004) Down's syndrome astrocytes have greater antioxidant capacity than euploid astrocytes. *Eur J Neurosci* **20**, 2355-2366.

[35] Dahlgren KN, Manelli AM, Stine WB, Baker LK, Krafft GA, LaDu MJ (2002) Oligomeric and Fibrillar Species of Amyloid-β peptides differentially Affect neuronal Viability. *J Biol Chem* **277**, 32046-32053.

[36] Prados J, Trobalon JB (1998) Locating an invisible goal in a water maze requires at least two landmarks. *Psychobiology* **26**, 42–48.

[37] Pertusa M, García-Matas S, Mammeri H, Adell A, Rodrigo T, Mallet J, Cristòfol R, Sarkis C, Sanfeliu C (2008) Expression of GDNF transgene in astrocytes improves cognitive deficits in aged rats. *Neurobiol Aging* **29**, 1366-1379.

[38] Damjanac M, Rioux Bilan A, Barrier L, Pontcharraud R, Anne C, Hugon J, Page G (2007) Fluoro-Jade B staining as useful tool to identify activated microglia and astrocytes in a mouse transgenic model of Alzheimer's disease. *Brain Res* **1128**, 40-49.

[39] Haghdoost-Yazdi H, Pasbakhsh P, Vatanparast J, Rajaei F, Behzadi G (2009) Topographical and quantitative distribution of the projecting neurons to main divisions of the septal area. *Neurol Res* **31**, 503-513.

[40] Nuutinen T, Huuskonen J, Suuronen T, Ojala J, Miettinen R, Salminen A (2007) Amyloid-β 1-42 induced endocytosis and clusterin/apoJ protein accumulation in cultured human astrocytes. *Neurochem Int* **50**, 540-547.

[41] Nielsen HM, Veerhuis R, Holmqvist B, Janciauskiene S (2009) Binding and uptake of Aβ1-42 by primary human astrocytes in vitro. *Glia* **57**, 978-988.

[42] Zhang Y, McLaughlin R, Goodyer C, LeBlanc A (2002) Selective cytotoxicity of intracellular amyloid β peptide$_{1\text{-}42}$ through p53 and Bax in cultured primary human neurons. *J Cell Biol* **156**, 519-529.

[43] Brera B, Serrano A, de Ceballos M (2000) β Amyloid peptides are cytotoxic to astrocytes in culture: a role for oxidative stress. *Neurobiol Dis* **7**, 395-405.

[44] Behl C, Davis JB, Lesley R, Schubert D (1994) Hydrogen peroxide mediates amyloid β protein toxicity. *Cell* **7**, 817-828.

[45] Abramov AY, Canevari L, Duchen MR (2003) Changes in intracellular calcium and glutathione in astrocytes as the primary mechanism of amyloid neurotoxicity. *J Neurosci* **23**, 5088-5095.

[46] Merrill, JE (1991) Effects of interleukin-1 and tumor necrosis factor-alpha on astrocytes, microglia, oligodendrocytes, and glial precursors in vitro. *Dev Neurosci* **13**, 130-137.

[47] Jalonen TO, Charniga CJ, Wielt DB (1997) β-Amyloid peptide-induced morphological changes coincide with increased K^+ and Cl^- channel activity in rat cortical astrocytes, *Brain Res* **746**, 85–97.

[48] Meske V, Hamker U, Albert F, Ohm TG (1998) The effects of β/A4-amyloid and its fragments on calcium homeostasis, glial fibrillary acidic protein and S100β staining, morphology and survival of cultured hippocampal astrocytes. *Neuroscience* **85**, 1151-1160.

[49] Liu W, Shafit-Zagardo B, Aquino DA, Zhao ML, Dickson DW, Brosnan CF, Lee SC (1994) Cytoskeletal alterations in human fetal astrocytes induced by interleukin-1β. *J Neurochem* **63**, 1625-1634.

[50] Wallace MN, Geddes JG, Farquhar DA, Masson MR (1997) Nitric oxide synthase in reactive astrocytes adjacent to β-amyloid plaques. *Exp Neurol* **144**, 266-272.

[51] Ayasolla K, Khan M, Singh AK, Singh I (2004) Inflammatory mediator and beta-amyloid (25-35)-induced ceramide generation and iNOS expression are inhibited by vitamin E. *Free Radic Biol Med* **37**, 325-338.

[52] Akama KT, Van Eldik LJ (2000) β-Amyloid stimulation of inducible nitric-oxide synthase in astrocytes is interleukin-1β- and tumor necrosis factor-α (TNFα)-dependent, and involves a TNFα receptor-associated factor- and NFκB-inducing kinase-dependent signaling mechanism. *J Biol Chem* **275**, 7918-7924.

[53] Ii M, Sunamoto M, Ohnishi K, Ichimori Y (1996) β-Amyloid protein-dependent nitric oxide production from microglial cells and neurotoxicity. *Brain Res* **720**, 93-100.

[54] White JA, Manelli AM, Holmberg KH, Van Eldik LJ, Ladu MJ (2005) Differential effects of oligomeric and fibrillar amyloid-beta 1-42 on astrocyte-mediated inflammation. *Neurobiol Dis* **18**, 459-465.

[55] Lee SC, Dickson DW, Liu W, Brosnan CF (1993) Induction of nitric oxide synthase activity in human astrocytes by interleukin-1β and interferon-γ. *J Neuroimmunol* **46**, 19-24.

[56] Liu J, Zhao ML, Brosnan CF, Lee SC (1996) Expression of type II nitric oxide synthase in primary human astrocytes and microglia: role of IL-1β and IL-1 receptor antagonist. *J Immunol* **157**, 3569-3576.

[57] Assis-Nascimento P, Jarvis KM, Montague JR, Mudd LM (2007) Beta-amyloid toxicity in embryonic rat astrocytes. *Neurochem Res* **32**, 1476-1482.

[58] Dodart JC, May P (2005) Overview on rodent models of Alzheimer's disease. *Curr Protoc Neurosci* Chapter 9, Unit 9.22.

[59] Begum AN, Yang F, Teng E, Hu S, Jones MR, Rosario ER, Beech W, Hudspeth B, Ubeda OJ, Cole GM, Frautschy SA (2008) Use of copper and insulin-resistance to

accelerate cognitive deficits and synaptic protein loss in a rat Aβ-infusion Alzheimer's disease model. *J Alzheimers Dis* **15**, 625-640.

[60] Malm T, Ort M, Tähtivaara L, Jukarainen N, Goldsteins G, Puoliväli J, Nurmi A, Pussinen R, Ahtoniemi T, Miettinen TK, Kanninen K, Leskinen S, Vartiainen N, Yrjänheikki J, Laatikainen R, Harris-White ME, Koistinaho M, Frautschy SA, Bures J, Koistinaho J (2006) β-Amyloid infusion results in delayed and age-dependent learning deficits without role of inflammation or beta-amyloid deposits. *Proc Natl Acad Sci USA* **103**, 8852-8857.

[61] Perry G, Friedman R, Shaw G, Chau V (1987) Ubiquitin is detected in neurofibrillary tangles and senile plaque neurites of Alzheimer disease brains. *Proc Acad Sci USA* **84**, 3033-3036.

[62] Song S, Jung YK (2004) Alzheimer's disease meets the ubiquitin-proteasome system. *Trends Mol Med* **10**, 565-570.

[63] Honda K, Smith MA, Zhu X, Baus D, Merrick WC, Tartakoff AM, Hattier T, Harris PL, Siedlak SL, Fujioka H, Liu Q, Moreira PI, Miller FP, Nunomura A, Shimohama S, Perry G (2005) Ribosomal RNA in Alzheimer disease is oxidized by bound redox-active iron. *J Biol Chem* **280**, 20978-20986.

[64] Smith MA, Harris PL, Sayre LM, Perry G (1997) Iron accumulation in Alzheimer disease is a source of redox-generated free radicals. Proc Natl Acad Sci USA **94**, 9866-9868.

[65] Smith MA, Hirai K, Hsiao K, Pappolla MA, Harris PL, Siedlak SL, Tabaton M, Perry G (1998) Amyloid-beta deposition in Alzheimer transgenic mice is associated with oxidative stress. *J Neurochem* **70**, 2212-2215.

[66] Abramov AY, Canevari L, Duchen MR (2004) Calcium signals induced by amyloid β peptide and their consequences in neurons and astrocytes in culture. *Biochim Biophys Acta* **1742**, 81-87.

[67] Heneka MT, O'Banion MK (2007) Inflammatory processes in Alzheimer's disease. *J Neuroimmunology* **184**, 69-91.

[68] Farfara D, Lifshitz V, Frenkel D (2008) Neuroprotective and neurotoxic properties of glial cells in the pathogenesis of Alzheimer's disease. *J Cell Mol Med* **12**, 762-780.

[69] Pallas M, Camins A, Smith MA, Perry G, Lee HG, Casadesus G (2008) From aging to Alzheimer's disease: unveiling "the switch" with the senescence-accelerated mouse model (SAMP8). *J Alzheimers Dis* **15**,615-624.

Figure legends

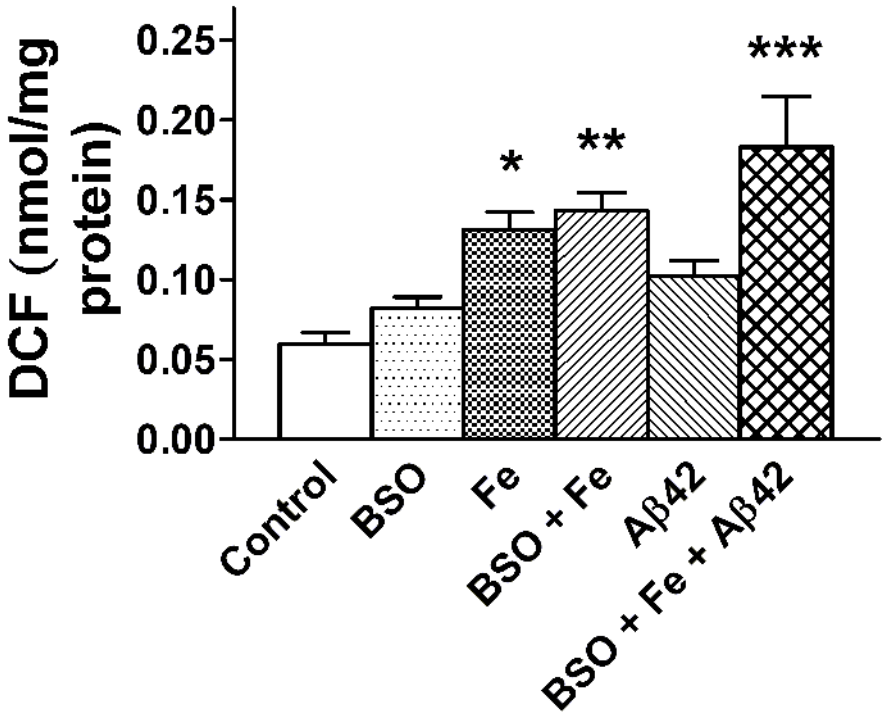

Fig. 1. Oxidative stress in human astrocyte cultures is increased by Aβ in pro-oxidant conditions. Treatment with $A\beta_{42}$ alone did not generate reactive oxygen species, but $A\beta_{42}$ potentiated the effect of pro-oxidant agents. Astrocytes were incubated with $A\beta_{42}$ 20 μM (Aβ42), $FeSO_4$ 25 μM (Fe) and buthionine sulfoximine 1mM (BSO) for 4 h at 37ºC. BSO was added 24 h before the addition of $A\beta_{42}$ and $FeSO_4$. The reactive oxygen species generation was assayed by dichlorofluorescein (DCF) formation. Results are shown as the mean ± SEM from duplicate determinations in four different cultures. Statistics: *$p<0.05$, **$p<0.01$ and ***$p<0.001$ as compared to control.

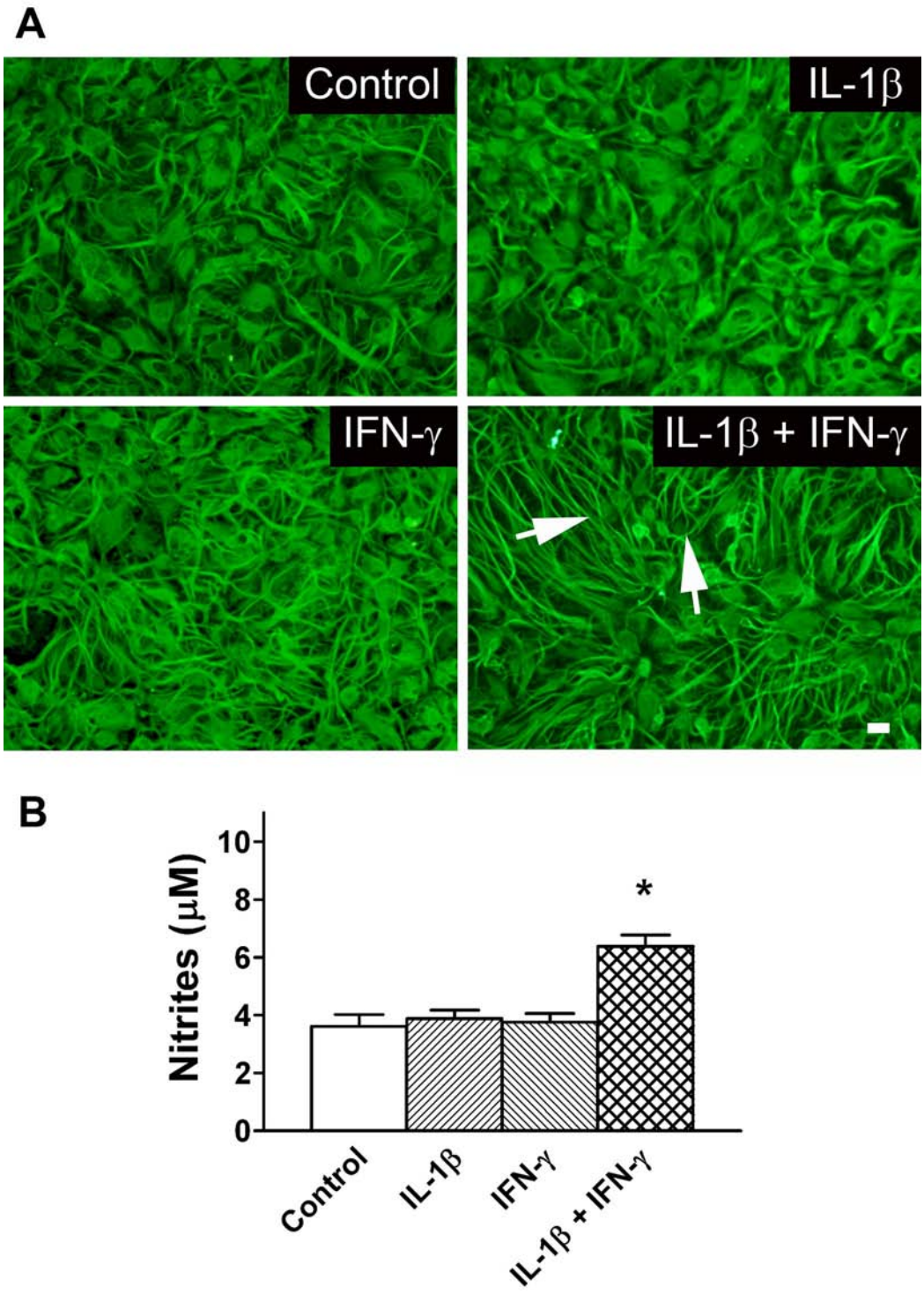

Fig. 2. Cytokine treatment causes activation of human astrocytes. Cultured astrocytes changed its polygonal shape to a smaller spherical body with long filamentous prolongations, known as stellate morphology, in the presence of active cytokines. Astrocyte morphology was visualized in astrocytes fixed with 4 % paraformaldehyde and stained with anti-GFAP antibody. Images show control astrocytes, and astrocytes

exposed to interleukin-1β 10 ng/ml (IL-1β), interferon-γ 10 ng/ml (IFN-γ) or both for 3 days. Arrows indicate long cytoplasmic processes characteristic of the activated stellate morphology. Scale bar: 20 μm. E) Nitrite accumulation in the respective culture media was measured using the Griess reagent. Results are shown as the mean ± SEM of four determinations from two different cultures. Statistics: *$p<0.001$ as compared to control.

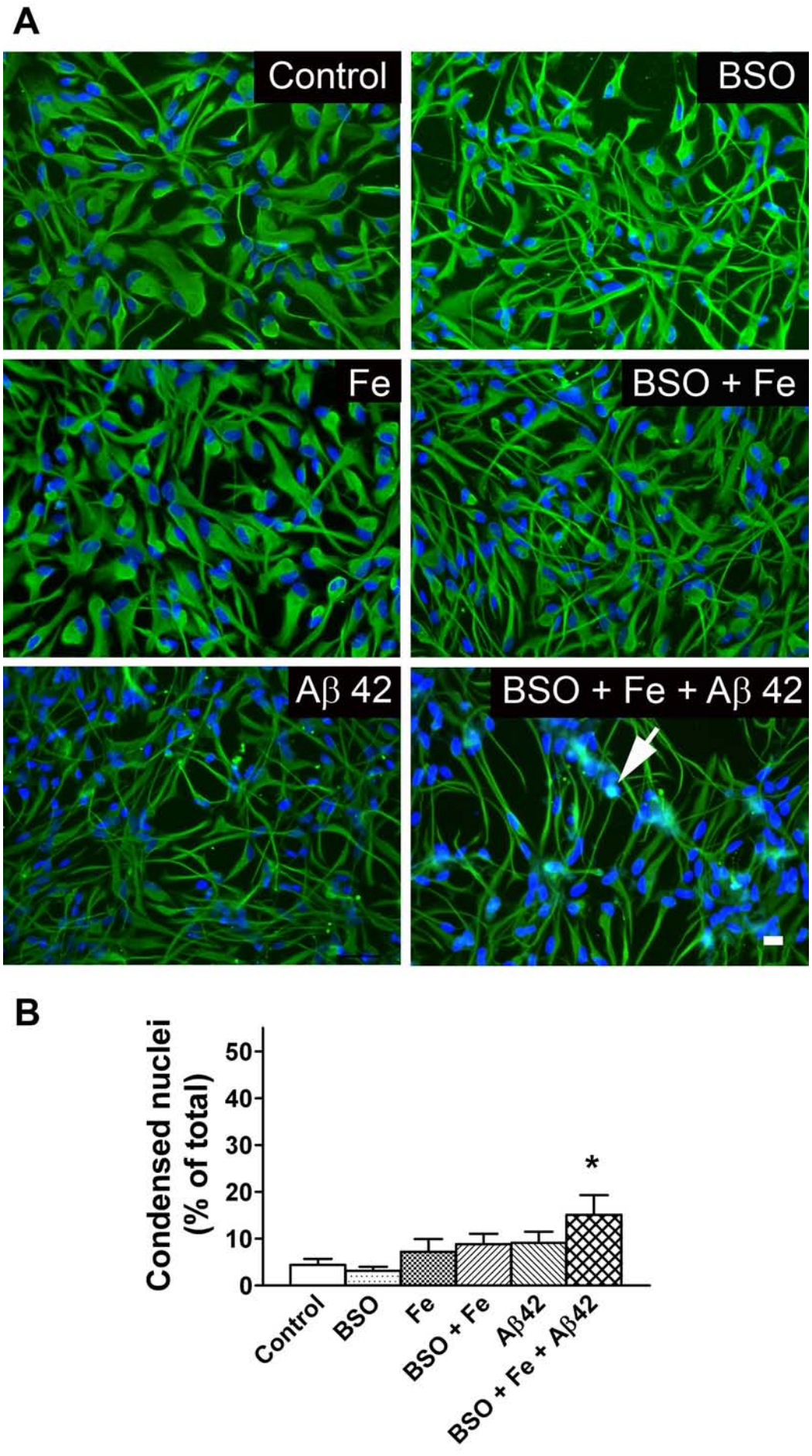
A
Control
BSO
Fe
BSO + Fe
Aβ 42
BSO + Fe + Aβ 42
B
Condensed nuclei
(% of total)
50
40
30
20
10
0
*
Control
BSO
Fe
BSO + Fe
Aβ42
BSO + Fe + Aβ42

Fig. 3. Pro-oxidant conditions trigger the toxic and inflammatory effects of Aβ in human astrocyte cultures. Treatment with $A\beta_{42}$ alone caused a barely distinguishable change to an activated morphology. However, the mixed treatment with $A\beta_{42}$ and pro-oxidant agents caused astrocyte activation and apoptosis. A) Astrocytes were stained with anti-GFPA antibody and nuclei were counterstained with bisbenzimide. Images show control astrocytes, as well as astrocytes exposed to $FeSO_4$ 10 μM (Fe) plus buthionine sulfoximine 1mM (BSO), those exposed to $A\beta_{42}$ 5 μM (Aβ42), and those exposed to both treatments, for 3 days. BSO was added 24 h before the addition of $A\beta_{42}$ and $FeSO_4$. Scale bar: 20 μm. B) The number of condensed and fragmented nuclei was recorded for the different treatments, as labeled in the graph. Results are shown as the mean ± SEM of three to five determinations from two different cultures. Statistics: *$p<0.05$ as compared to control.

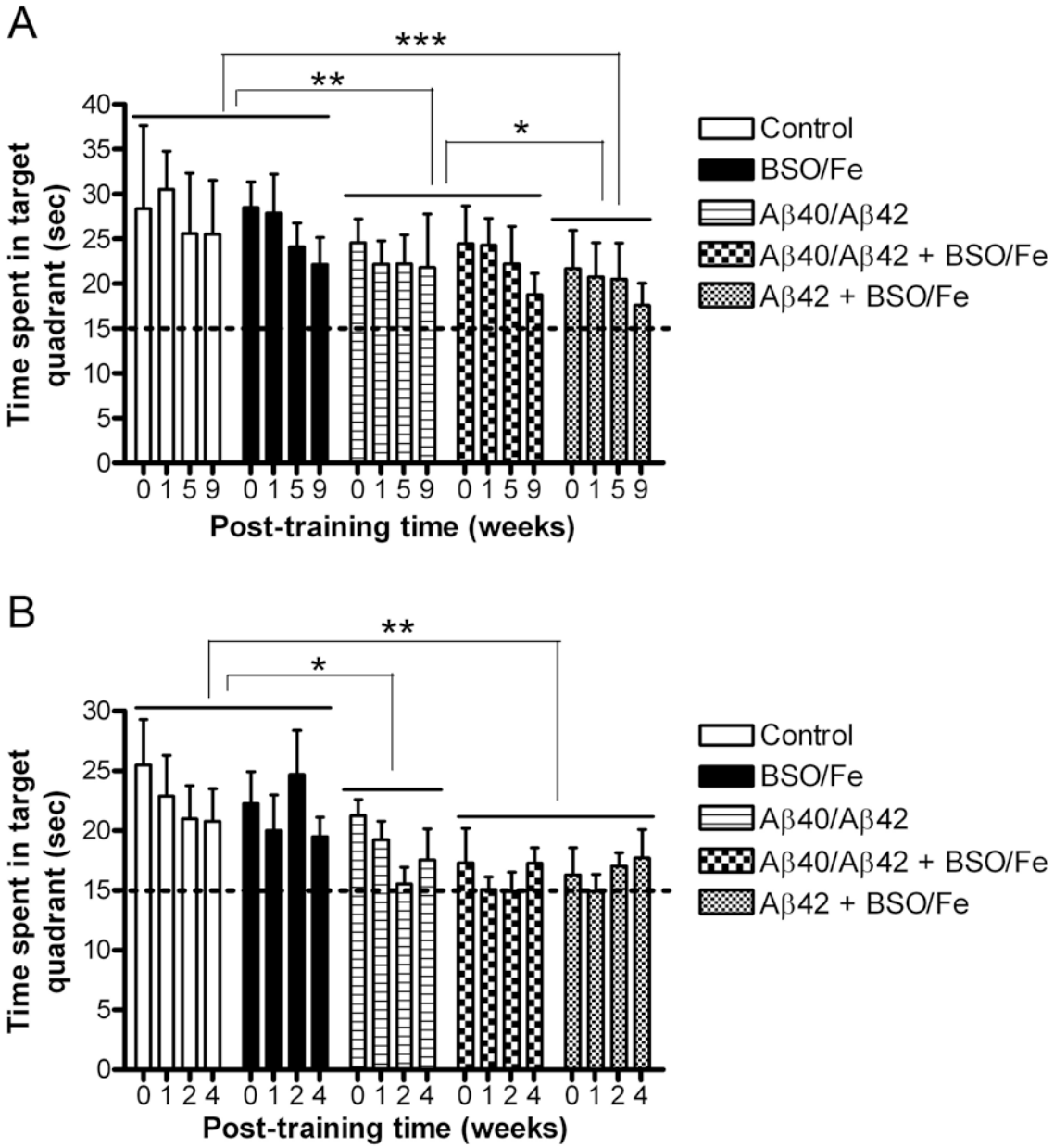

Fig. 4. In vivo treatment with Aβ causes a decreased cognitive capacity that is potentiated by pro-oxidant agents in adult rats. Cognitive behavioral testing in the Morris water maze of rats administrated with Aβ and a pro-oxidant treatment showed long term cognitive loss. Pro-oxidant agents alone did not induce any effect on rat behavior. Rats were previously administrated icv for 4 weeks with: I, a vehicle (Control); II, a pro-oxidant treatment of 4.48 mg buthionine sulfoximine and 0.47 mg $FeSO_4$ heptahydrate (BSO/Fe); III, a mixture of 20 µg $A\beta_{40}$ and 30 µg $A\beta_{42}$ ($A\beta_{40}/A\beta_{42}$); IV, pro-oxidant treatment plus $A\beta_{40}$ and $A\beta_{42}$ mixture ($A\beta_{40}/A\beta_{42}$ + BSO/Fe); and V, a pro-oxidant plus a high $A\beta_{42}$ treatment of 50 µg ($A\beta_{42}$ + BSO/Fe).

A) Probe trials performed after a 6 day acquisition period (week 0) and thereafter at 1, 5 and 9 weeks later. An initial stronger effect was seen in the group V as compared to the group IV. B) Probe trials performed after a reversal platform acquisition, initiated 3 weeks after the previous behavioral study at the end of acquisition (week 0) and 1, 2 and 4 weeks later. In the long term, both groups dosed with Aβ plus pro-oxidants (IV and V) showed similarly high deleterious effects on cognition. Dotted lines indicate chance performance. Statistics: *p<0.05, **p<0.01, ***p<0.001 as compared to the indicated experimental group.

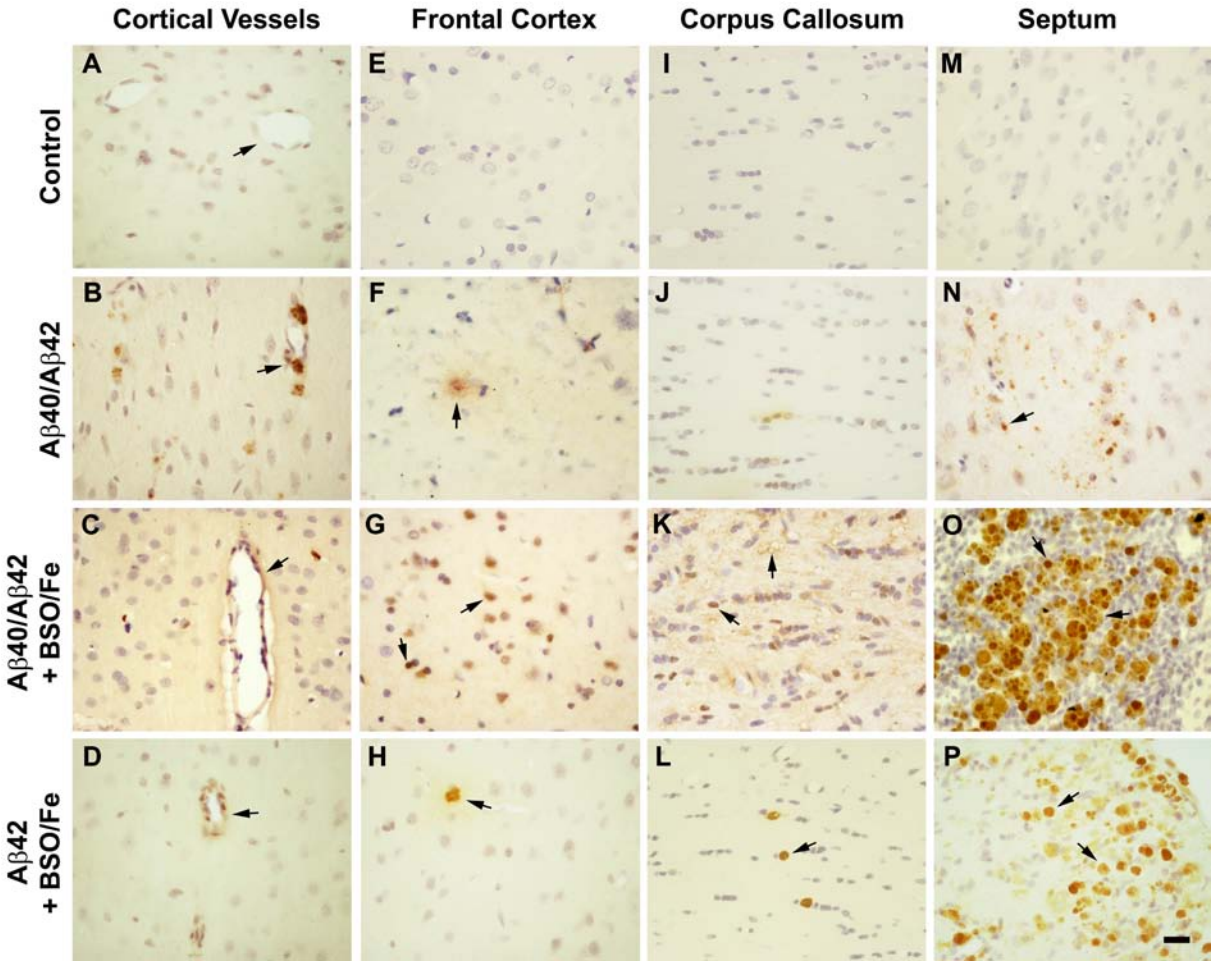

Fig. 5. Pro-oxidant agents potentiate brain Aβ accumulation. Aβ precipitates were found scattered in the brain tissue near the ventricular area where it was infused. Vessels also stained positive for Aβ. The long term Aβ accumulation was higher in the groups simultaneously dosed with pro-oxidant agents. Immunohistochemistry was performed with anti-Aβ antibody 4G8 and nuclei were lightly counterstained with hematoxylin. A-D) Representative images of cerebral cortical capillary blood vessels in animals

sacrificed after the infusion period. E-P) Representative images of frontal cortex, corpus callosum and septum of animals sacrificed at the end of the study, 4 months post treatment. Arrows point to Aβ deposits and Aβ positive capillary vessels. For details of treatment groups see the legend to Fig. 4. Scale bar = 20 μm.

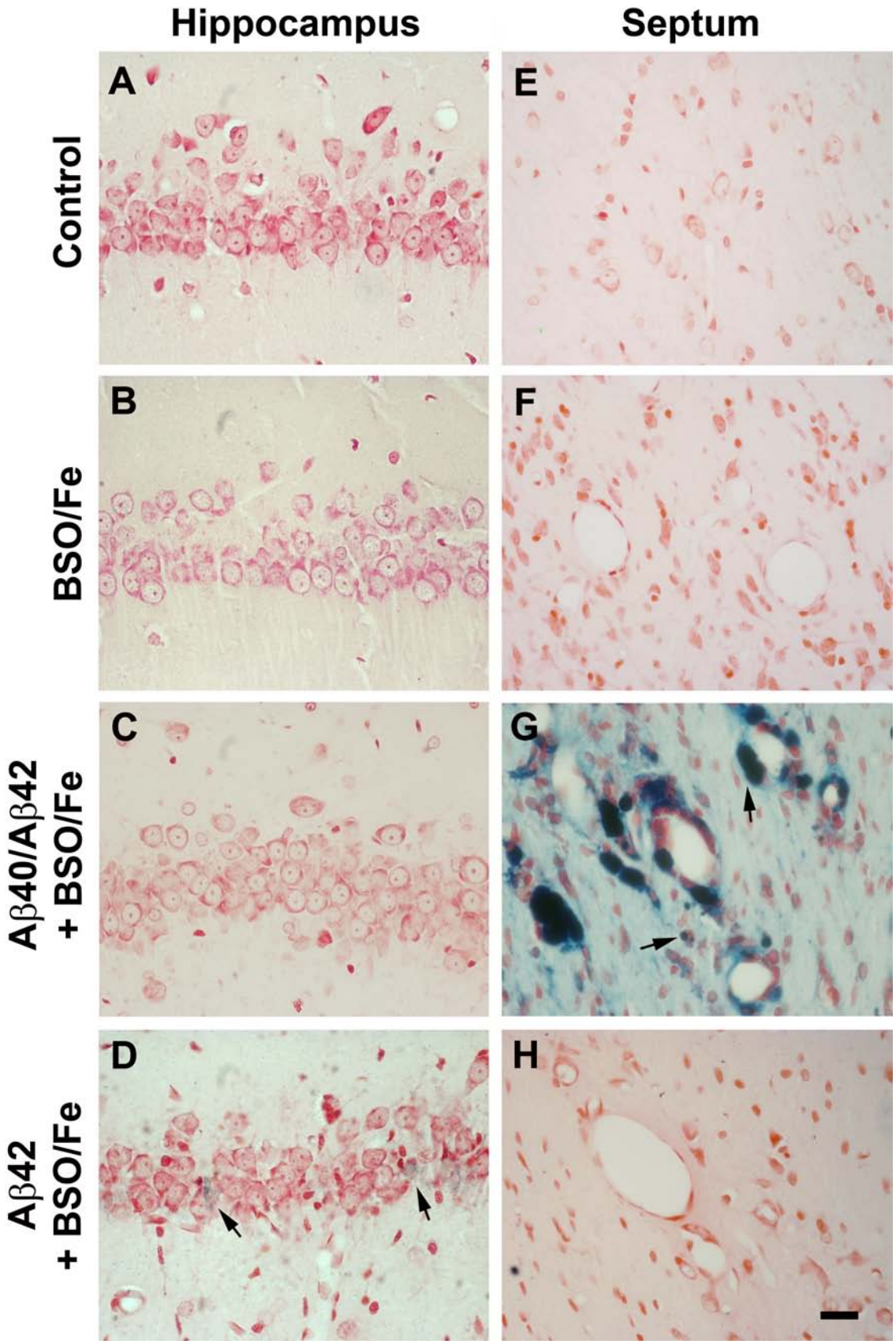
Hippocampus
Septum
Control
BSO/Fe
Aβ40/Aβ42
+ BSO/Fe
Aβ42
+ BSO/Fe
A
B
C
D
E
F
G
H

Fig. 6. Brain iron accumulation was caused by Aβ treatment. Accumulated ferric iron was barely present in the brain rat after the infusion period and only in the group dosed with $A\beta_{42}$ + BSO/Fe. However, 4 months later, the rats dosed with $A\beta_{40}/A\beta_{42}$ + BSO/Fe showed extensive iron accumulation. Histochemistry was performed with Pearl's Prussian blue and tissue was counterstained with neutral red. A-D) Pyramidal layer of hypocampus CA1 of rats sacrificed at the end of the infusion period. E-H) Septum of rats sacrificed at the end of the study, 4 months later. Arrows point to intra and extracellular precipitates. For details of treatment groups see the legend to Fig. 4. Scale bar = 20 μm in A- D and 40 μm in E-H.

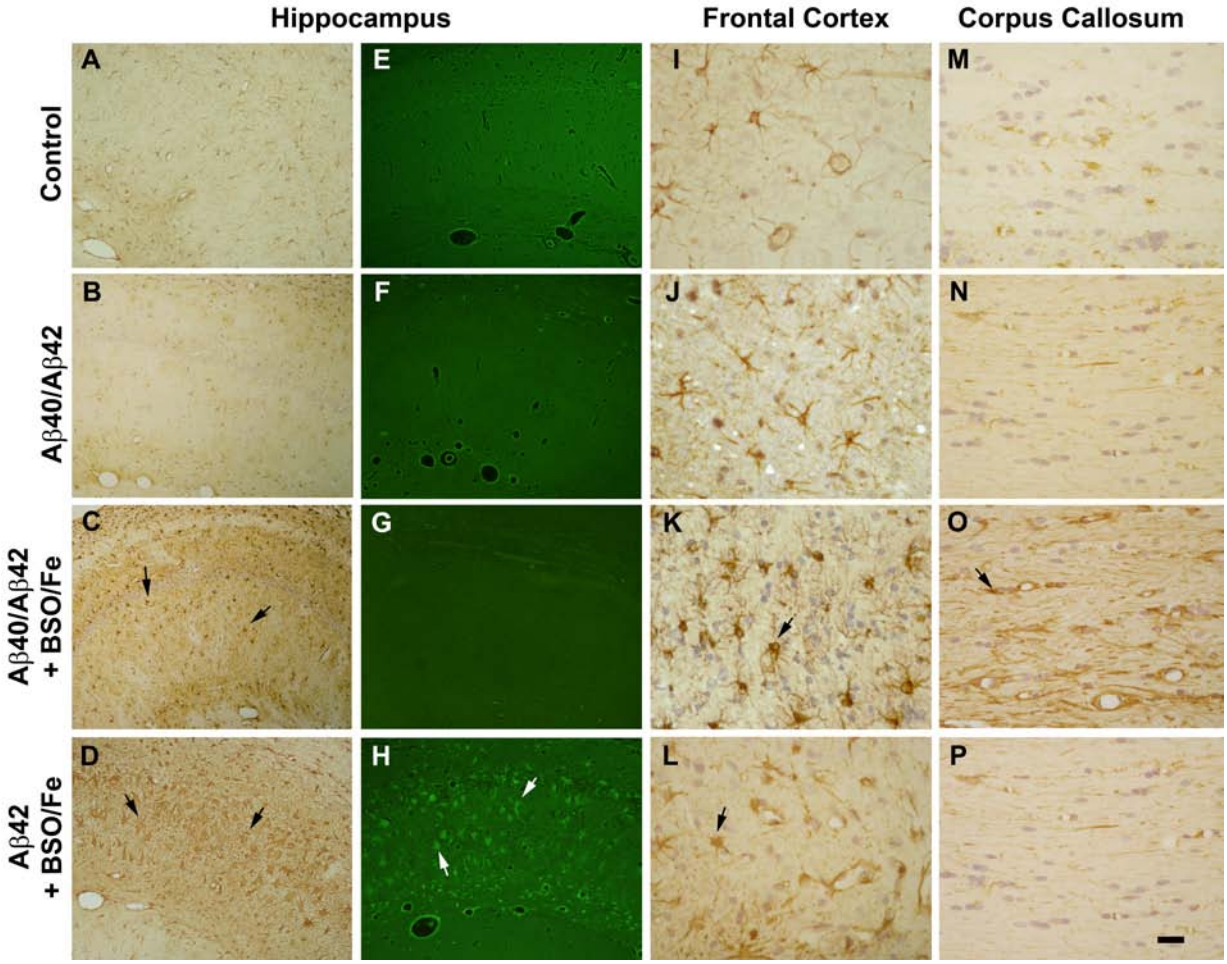

Fig. 7. Pro-oxidant agents potentiate astrocyte activation induced by Aβ treatment. Immediately after treatment, the higher astrocyte reactivity was caused by $A\beta_{42}$ + BSO/Fe, where astrocytes also stained positive for Fluoro-Jade B. Long term reactive astrocytes were mainly observed in rats treated with $A\beta_{40}/A\beta_{42}$ + BSO/Fe. A-D) Images of immunohistochemistry with anti-GFPA antibody and light counterstain with

hematoxylin in hippocampus Ammon's horn of rats sacrificed immediately after the infusion treatment. E-H) Fluoro-Jade B fluorescence staining of the same brain area and treatment groups than the previous images, as indicated. I-P) GFAP immunostaining in frontal cortex and corpus callosum of rats sacrificed at the end of the study, 4 months post treatment. Arrows point to reactive astrocytes. For details of treatment groups see the legend to Fig. 4. Scale bar = 80 μm in A-H and 20 μm in I-P.

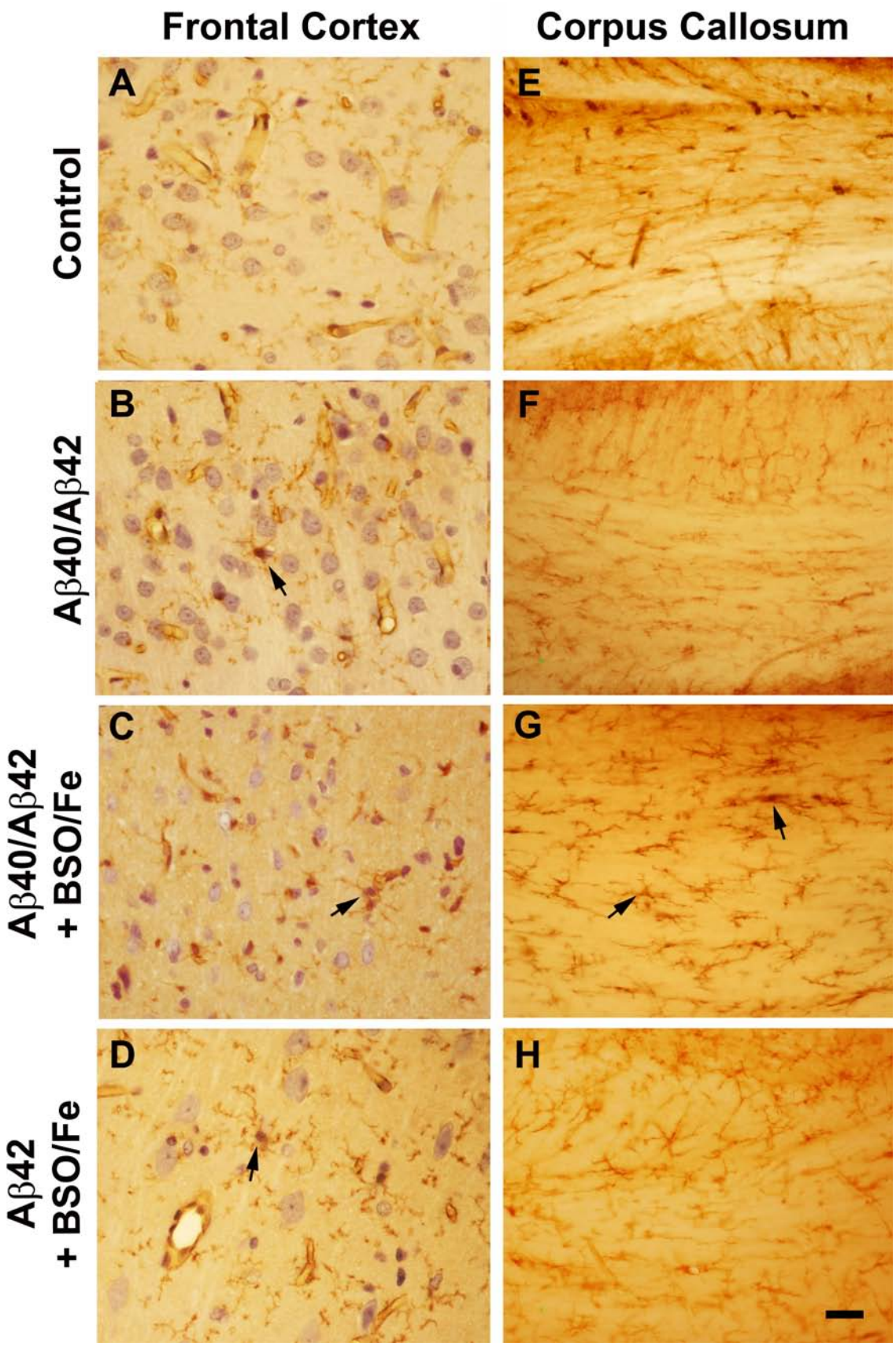
Frontal Cortex
Corpus Callosum
Control
Aβ40/Aβ42
Aβ40/Aβ42 + BSO/Fe
Aβ42 + BSO/Fe
A
B
C
D
E
F
G
H

Fig. 8. Pro-oxidant agents potentiate microglia activation induced by Aβ treatment. Treatment with $A\beta_{40}/A\beta_{42}$ + BSO/Fe caused microglia reactivity that was maintained up to the end of the study, 4 months after treatment. The other Aβ treatments assayed caused short time reactivity. A-D) Microglia staining with *Lycopersicum esculentum lectin* hystochemistry and light counterstain with hematoxylin in frontal cortex of rats sacrificed immediately after treatment. E-H) Immunostaining of reactive microglia with anti-OX42 in the corpus callosum of rats sacrificed at the end of the study. Arrows indicate reactive microglia. For details of treatment groups see the legend to Fig. 4. Scale bar = 20 μm in A-D and 40 μm in E-H.

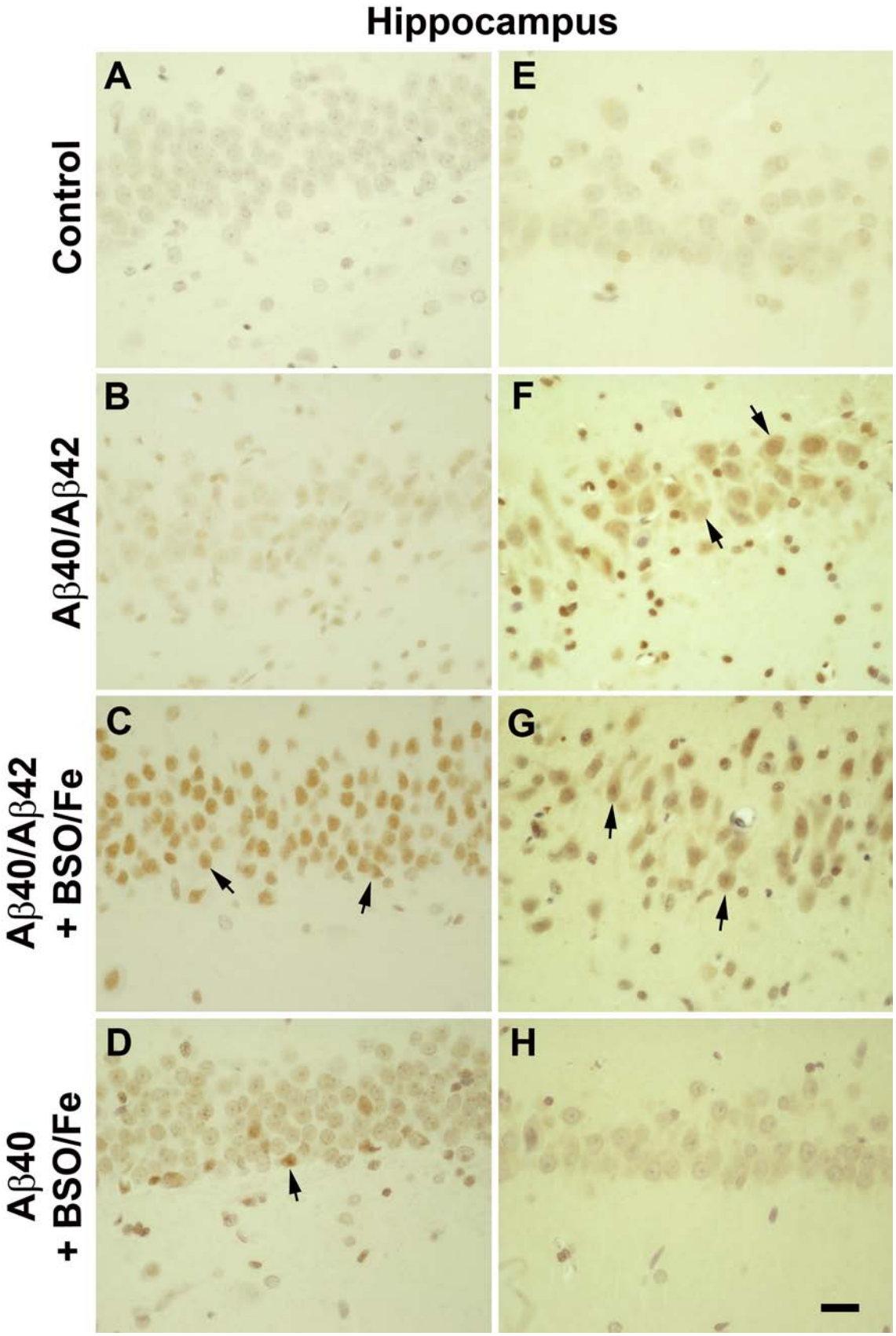

Fig. 9. Brain neurons suffer a delayed damage after Aβ and pro-oxidant agent treatment. Neuronal damage was not detected histologically in the early sacrificed rats, but only at

the long term period assayed at 4 months post treatment. A-D) DNA oxidation, as indicated by staining with anti-8-OHdG antibody, was caused by $A\beta_{40}/A\beta_{42}$ + BSO/Fe and in minor degree by $A\beta_{42}$ + BSO/Fe. E-H) Proteasome system dysfunction, as indicated by anti-ubiquitin antibody staining of intraneuronally accumulated ubiquitin, was caused by $A\beta_{40}/A\beta_{42}$ in the presence or absence of pro-oxidants. After immunohistochemistry, tissue was lightly counterstained with hematoxylin. Arrows point to damaged pyramidal neurons. For details of treatment groups see the legend to Fig. 4. Scale bar = 20 μm.